Ultramiscoscopy 3 (1979) 391–395

MONTE CARLO ELECTRON TRAJECTORY SIMULATION OF BEAM SPREADING IN THIN FOIL TARGETS

Dale E. NEWBURY and Robert L. MYKLEBUST
National Bureau of Standards, Washington, DC 20234, USA

1. Introduction

The determination of the volume of electron excitation in a foil sample is an important problem in establishing limits of spatial resolution in analytical electron microscopy. Ideally, the excitation volume would be a cylinder whose diameter is that of the incident beam and whose height is the specimen thickness. However, the phenomenon of beam spreading occurs, primarily as a result of elastic scattering events, causing the electrons to deviate significantly from their original trajectories defined by the initial beam parameters. A number of experiments have been carried out to directly measure the interaction volume in a thin film [1–3]. In addition, several theoretical methods can be used to study the problem of beam spreading: (a) a simple analytic approach based on single scattering events; (b) solution of a rigorous transport equation; and (c) Monte Carlo electron trajectory simulation. To date, methods (a) and (c) have been applied to the problem of beam spreading and will be considered here.

2. Analytic approach

Goldstein et al. [4] have provided a very useful analytical approach to provide an estimate of beam spreading for a point beam incident normal to a foil. These authors assumed that a condition of single scattering exists with scattering described by the screened Rutherford model:

$$p(>\phi) = 9.76 \times 10^3 (Z^2/AE^2) \cot^2(\tfrac{1}{2}\phi)\, \rho t \,, \qquad (1)$$

where p is the probability of scattering through an angle greater than ϕ, Z is the atomic number, A is the atomic weight (g/mol), E is the electron energy (keV), ρ is the density (g/cm^3), and t is the foil thickness (cm). Defining the extent of beam spreading by the volume containing 90% of the trajectories, these authors solved eq. (1) for the angle $\phi_{0.1}$ containing all but the last 10% of the scattering events. The approximation $\cot(\frac{1}{2}\phi) = 2/\phi$ was employed, and the equation was solved in terms of the thickness, t,

$$t = 2.56 \times 10^{-6}\, AE^2 \phi_{0.1}^2 / \rho Z^2 \,. \qquad (2)$$

Beam broadening was defined as the diameter of the base of a cone, b, whose semi-angle corresponded to the value of $\phi_{0.1}$ and whose apex was set at the center of the foil. The approximation $\phi_{0.1} = \tan \phi_{0.1} = \frac{1}{2} b / \frac{1}{2} t$ was employed. Substituting $\phi_{0.1} = b/t$ in eq. (2), the following equation was obtained to describe beam broadening:

$$b = 6.25 \times 10^2 (\rho/A)^{0.5} (Z/E)\, t^{1.5} \,, \qquad (3)$$

where b is the broadening (cm) experienced by a point beam of energy E (keV) in traversing a foil of thickness t (cm) having a density ρ (g/cm^3), atomic weight A (g/mol), and atomic number, Z. Values calculated by these authors for several elements and foil thicknesses are listed in table 1.

Eq. (3) is only valid for a single scattering situation. When multiple scattering occurs, the possible cumulative effect of several scattering events on the net scattering angle leads to a larger value of beam broadening than that predicted by eq. (3). Moreover, the equation describes a point beam incident normally on a foil. The interesting case of a finite beam with a distribution of intensity incident on a tilted foil is difficult to describe analytically.

Table 1
Electron beam spreading in thin foils calculated with the analytical model of Goldstein et al. [4]. E = 100 keV. Broadening in Å, defined as diameter of cylinder containing 90% of X-ray generation. Point beam

Element	Foil thickness (Å)				
	100	500	1000	3000	5000
carbon	1.6Å	18	51.3	267	574
aluminum	2.6	29	81.2	422	909
copper	6.8	76	214	1117	[a]
gold	15.5	173	[a]	[a]	[a]

[a] Model breaks down.

3. Monte Carlo electron trajectory simulation

In a Monte Carlo electron trajectory simulation, the path of an individual electron is calculated in a stepwise manner through the solid as the electron undergoes elastic and inelastic scattering. The distance between scattering events, the scattering angles, and the amount of energy loss are calculated from realistic physical models. Random numbers are used to distribute the choices for these parameters over their respective ranges so as to accurately represent the relative probabilities for each process. Because of the large number of possible choices for these parameters and the combinations thereof along a trajectory, a single trajectory calculation does not adequately describe the beam–specimen interaction. To provide statistically valid results, a large number of trajectories, typically one thousand or more, must be calculated. Along a particular trajectory, it may be necessary to calculate several hundred scattering acts. The Monte Carlo simulation thus requires much computer time.

By its very nature, the Monte Carlo electron trajectory simulation is extremely well suited for application to the problem of beam spreading in a thin foil. The coordinates of the position of the electron after each scattering act are calculated, hence spatial distributions of events of interest such as X-ray generation can be readily calculated. Kyser and Geiss [5] have applied the Monte Carlo technique to the beam spreading problem and have reported X-ray generation distributions for gold and copper foils of various thicknesses at a beam energy of 100 keV.

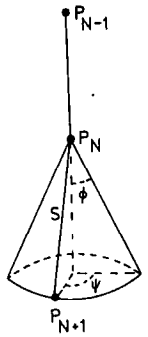

Fig. 1. Fundamental calculational element of Monte Carlo electron trajectory simulation.

The details of Monte Carlo electron trajectory simulation methods can be found in the literature [6–8]. In this report, the necessary equations for a simple Monte Carlo scheme which is capable of simulating beam spreading will be given.

1. An orthogonal coordinate system is established which is fixed to the specimen. The x–y plane is the plane of the specimen; the x-axis is parallel to the tilt axis; and the positive z-axis lies into the specimen.

2. A finite beam size with a Gaussian intensity distribution along a diameter is obtained from the following equations which give the beam impact points at the specimen surface:

$$x = \cos(R_L \pi)\, R_G \Sigma\,,$$
$$y = \sin(R_L \pi)\, R_L \pi)\, R_G \Sigma / \cos\theta\,, \qquad (4)$$
$$z = 0\,,$$

where R_L is a uniformly distributed random number ($-1 \leqslant R_L \leqslant 1$), R_G is a random number with Gaussian distribution, Σ is the standard deviation of the distribution (cm), and θ is the angle of specimen tilt.

3. The fundamental repetitive calculational element of the Monte Carlo simulation is illustrated in fig. 1. In taking the electron from point P_N to point P_{N+1} we require a step length, S, a scattering angle ϕ, and an azimuthal angle ψ. ϕ will be calculated on the basis of elastic scattering only. Inelastic scattering leads to only slight angular deviations. The total Rutherford scattering cross section is used to model elastic scattering:

$$\sigma_E = 5.21 \times 10^{-21} \frac{Z^2}{E^2} \frac{4\pi}{\alpha(1+\alpha)} \left(\frac{E + m_0 c^2}{E + 2m_0 c^2} \right)^2 , \qquad (5)$$

where σ_E is the total scattering cross section (cm^2), E is the electron energy (keV), α is a screening factor, and the final factor in parentheses corrects for relativistic effects [9]. For convenience, the factor m_0c^2 corresponds to 511 keV for an electron. The screening factor α has been given by Bishop [10] as:

$$\alpha = 3.4 \times 10^{-3} Z^{0.67}/E \,, \tag{6}$$

where E is in keV. From the total cross section, a mean free path between scattering events can be calculated:

$$\lambda = A/N_A \rho \sigma_E \,, \tag{7}$$

where λ is the mean free path (cm), A is the atomic weight (g/mol), N_A is Avogadro's number (at/mol), ρ is the density (g/cm^3), and σ_E has the dimensions (scattering events/el/at/cm^2). Note that this length is a mean free path. A step length is calculated from this mean free path by allowing for a statistical distribution [9]:

$$S = -\lambda \log_e |R_L| \,. \tag{8}$$

The differential form of the Rutherford cross section is also needed:

$$\frac{d\sigma}{d\Omega} = 5.21 \times 10^{-21} \frac{Z^2}{E^2} \left(\frac{E + m_0c^2}{E + 2m_0c^2} \right)^2 \times (\sin^2(\tfrac{1}{2}\phi) + \alpha)^{-2} \,. \tag{9}$$

The ratio of the differential cross section to the total cross section can be integrated over all scattering angles to generate an appropriate function for selection of the scattering angles by random numbers:

$$R = \int_\Omega \frac{\sigma'(\phi)}{\sigma_E} \, d\Omega \,. \tag{10}$$

This integration yields the following equation for the scattering angles:

$$\cos\phi = 1 - [2\alpha R_L/(1 + \alpha - R_L)] \,. \tag{11}$$

The azimuthal angle, ψ, is found from

$$\psi = 2\pi R_L \,. \tag{12}$$

With the electron at a point P_N, (X_N, Y_N, Z_N), a new set of scattering parameters (S, ϕ, ψ) is calculated from eqs. (8), (11), and (12). The coordinates of the new point, P_{N+1}, are given by the following set of equations [11]:

$$X_{N+1} = X_N + SA \cos\phi + S \cos\Delta \sin\phi \cos(R_L 2\pi) + SB \cos\Gamma \sin\phi \sin(R_L 2\pi) \,, \tag{13}$$

$$Y_{N+1} = Y_N + SB \cos\phi + S \sin(R_L 2\pi) \times (C \cos\Delta - A \cos\Gamma) \tag{14}$$

$$Z_{N+1} = Z_N + SC \cos\phi + S \cos\Gamma \cos(R_L 2\pi) + S \sin(R_L 2\pi)(-B \cos\Delta) \,, \tag{15}$$

where A, B, C are the direction cosines of the segment of the trajectory preceding point P_N and $\Delta = \arctan(-A/C)$ and $\Gamma = \arctan(-C/A)$. For the initial beam electron, the direction cosines are defined by the beam relative to the coordinate axes. ϕ is taken as zero prior to the first scattering act. The initial scattering event occurs after the electron travels a distance S into the film given by (8).

Energy loss along the trajectory is calculated by taking the segment length multiplied by the rate of energy loss with distance traveled given by the Bethe equation:

$$E = S(dE/ds) \tag{16}$$

$$dE/ds = -7.85 \times 10^4 (\rho Z/EA) \times \log_e(1.166\, E/J) \tag{17}$$

where dE/ds is the rate of energy loss (keV/cm) and J is the mean ionization potential. J can be calculated by the Berger–Seltzer [12] equation:

$$J = 9.76\, Z + 58.5\, Z^{-0.19} (\text{eV}) \,. \tag{18}$$

Because of the small mass thickness of the foils to be studied, the energy loss can be disregarded without much loss of accuracy, since the total energy change is only a few percent while traveling through the foil.

4. Calculation of beam spreading

Since the beam energies used for analytical electron microscopy are of the order of 100 keV and the energy loss during transmission is only a few percent at most, the cross section for inner shell ionization leading to X-ray formation is essentially constant for all points in the interaction volume. The distribution of X-ray generation events is thus identical to the

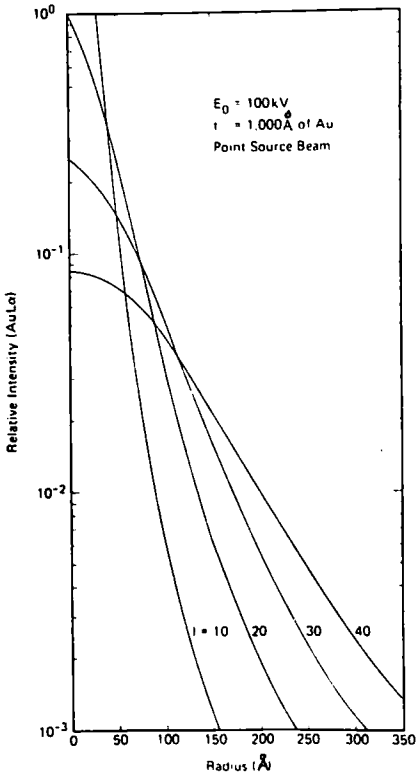

Fig. 2. Beam spreading in gold plotted at depths of 250, 500, 750, and 1000 Å. From Kyser and Geiss [5].

distribution of electron trajectories. Several types of electron distributions can be constructed. The cumulative radial distribution can be calculated from the magnitude of the radial position vector, $r = (x^2 + y^2)^{0.5}$, for each scattering event. This distribution can be summed over all values of z, or the foil can be considered to be divided into layers. Kyser and Geiss [5] graphically illustrated such progressive beam spreading through the foil with a Monte Carlo simulation, fig. 2.

With the present Monte Carlo simulation, the cumulative radial distribution function has been determined for the same materials and conditions listed in table 1. The diameter of a cylinder containing 90% of the X-ray generation events is listed in table 2. Comparing the Monte Carlo results of table 2 with the results calculated with the analytical model [4], it can be seen that the Monte Carlo values are slightly higher than the analytical model calculations for the 100 Å thick foil. For thicker foils, the Monte

Table 2
Electron beam spreading in thin foils calculated with Monte Carlo electron trajectory simulation. E = 100 keV. Broadening in Å, defined as diameter of cylinder containing 90% of X-ray generation. Point beam; precision ±10%

Element	Foil thickness (Å)				
	100	500	1000	3000	5000
carbon	2.2Å	19	41	160	330
aluminum	4.1	30	76	300	664
copper	7.8	58	175	970	2440
gold	17.1	150	522	5990	17250

Carlo values are significantly less than the values predicted by the analytical model, with the deviations as high as 40% for the thickest foils. This result is contrary to what would be expected, since the analytical model does not consider multiple scattering whereas the Monte Carlo simulation does. The difference is probably a result of the choice of the particular forms of the elastic scattering cross sections used in the analytical model and the Monte Carlo simulation. Additional Monte Carlo calculations will be made with Mott cross sections, as suggested by Reimer and Krefting [9].

The Monte Carlo simulation is especially well adapted to an examination of the tail of the beam spreading distribution. Table 3 contains values calculated for the diameter of a cylinder containing 99% of the X-ray generation events. This diameter is larger than the corresponding value for the 90% cylinder by a factor ranging from about three to ten, depending on material and thickness. For elements of high

Table 3
Electron beam spreading in thin foils calculated with Monte Carlo electron trajectory simulation. E = 100 keV. Point beam. Diameter in Å of cylinder containing 99% of generated X-rays. Precision ±20%

Element	Foil thickness (Å)				
	100	500	1000	3000	5000
carbon	12Å	60	153	650	1570
aluminum	20	114	240	1260	4800
copper	27	350	930	12200	32400
gold	66	2390	5550	27000	40140

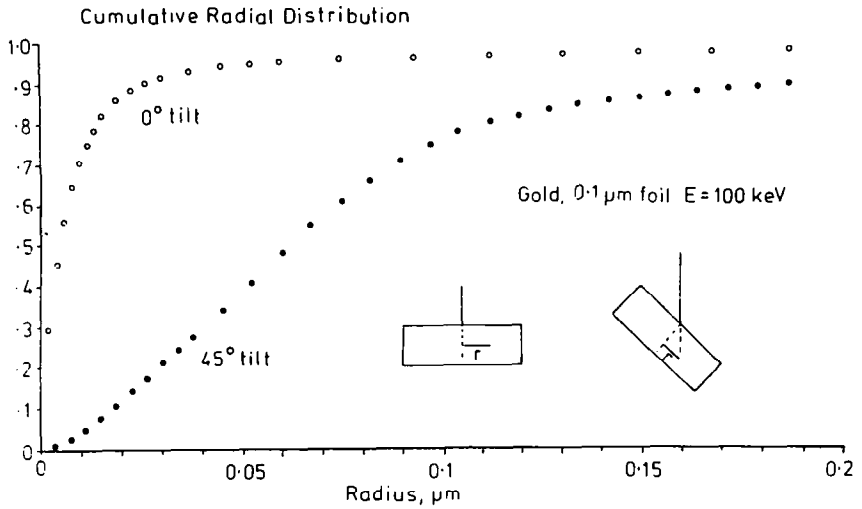

Fig. 3. Comparison of beam spreading for normal incidence and a specimen tilt of 45°. Gold foil, point beam, 100 keV.

atomic number or thick foils, 10% of the generated X-rays are spread over a very large radius. Clearly, this enormous tailing effect can have considerable implications for microanalysis situations where minor constituents are to be determined, as in the case of determining a minor constituent in a precipitate when that same constituent is found in the surrounding matrix.

The case of beam spreading in a tilted specimen can also be treated conveniently with the Monte Carlo simulation. The cumulative radial distribution functions for a normal incidence specimen and a tilted specimen are compared in fig. 3. In both cases, the distribution is determined relative to a line drawn normal to the surface at the beam impact point. At normal incidence, 90% of the X-ray intensity is contained within a radius of 260 Å, whereas only 17% of the intensity is contained within that radius for the tilted specimen. The 90% condition is not reached for the tilted specimen until the radius is extended to about 1900 Å. The interaction volume for the tilted specimen is strongly asymmetric due to the tendency for forward scattering.

Monte Carlo electron simulation techniques are very powerful tools for the study of beam spreading in thin foils. In addition to the calculations illustrated above, the Monte Carlo simulation can be extended to calculate X-rays generated in a discrete object contained within a foil. Since the history of each electron is known, multiple scattering can be readily studied and separated from single event high angle scattering. In applying the Monte Carlo simulation, however, it must be remembered that the simulation can be no better than the quality of the scattering models and approximations used in its construction.

References

[1] K.E. Easterling, J. Mat. Sci. 12 (1977) 857.
[2] R.G. Faulkner, T.C. Hopkins and K. Norrgard, X-ray Spectry 6 (1977) 73.
[3] L.S. Lin, J.I. Goldstein and D.B. Williams, Geochim. Cosmochim Acta 41 (1977) 1861.
[4] J.I. Goldstein, J.L. Costley, G.W. Lorimer and S.J.B. Reed, SEM/1977 1 (1977) 315.
[5] D. Kyser and R. Geiss, 12th Ann. Conf. Microbeam Analysis Society, Boston (1977) 110A.
[6] M. Berger, in Methods in Computational Physics, vol. 1, eds. B. Alder, S. Fernback and M. Rotenberg (Academic Press, New York, 1963).
[7] R. Shimizu, Y. Kataoka, T. Ikuta, T. Koshikawa and H. Hashimoto, J. Phys. D9 (1976) 101.
[8] Use of Monte Carlo Calculations in Electron Probe Microanalysis and Scanning Electron Microscopy, eds. K.F.J. Heinrich, D.E. Newbury and H. Yakowitz, NBS SP 460 (Washington, 1976).
[9] L. Reimer and E.R. Krefting, ibid., NBS SP 460, p. 45.
[10] H.E. Bishop, ibid., NBS SP 460, p. 5.
[11] R.L. Myklebust, D.E. Newbury and H. Yakowitz, ibid., NBS SP 460, p. 105.
[12] M.J. Berger and S.M. Seltzer, National Academy of Science – National Research Council Publ. 1133 (Washington, 1964) 205.